Long non-coding RNA BC168687 small interfering RNA reduces high glucose and high free fatty acid-induced expression of P2X$_7$ receptors in satellite glial cells

CHENG-LONG LIU[1], ZE-YU DENG[1], ER-RONG DU[1] and CHANG-SHUI XU[1,2]

[1]Department of Physiology, Basic Medical College of Nanchang University; [2]Jiangxi Provincial Key Laboratory of Autonomic Nervous Function and Disease, Nanchang University, Nanchang, Jiangxi 330006, P.R. China

Abstract. Purinergic signaling contributes to inflammatory and immune responses. The activation of the P2X purinoceptor 7 (P2X$_7$) in satellite glial cells (SGCs) may be an essential component in the promotion of inflammation and neuropathic pain. Long non-coding RNAs (lncRNAs) are involved in multiple physiological and pathological processes. The aim of the present study was to investigate the effects of a small interfering RNA for the lncRNA BC168687 on SGC P2X$_7$ expression in a high glucose and high free fatty acids (HGHF) environment. It was demonstrated that BC168687 small interfering (si)RNA downregulated the co-expression of the P2X$_7$ and glial fibrillary acidic protein and P2X$_7$ mRNA expression. Additionally, HGHF may activate the mitogen-activated protein kinase signaling pathway by increasing the release of nitric oxide and reactive oxygen species in SGCs. Taken together, these results indicate that silencing BC168687 expression may downregulate the increased expression of P2X$_7$ receptors in SGCs induced by a HGHF environment.

Introduction

Type 2 diabetes mellitus (T2DM) is a prevalent endocrine and metabolic disease. Changes in life style and accelerations in the aging process have contributed to the increasing prevalence of T2DM. It is a chronic non-communicable disease that particularly affects those with cardiovascular or cerebrovascular diseases (1-3). In addition, diabetic neuropathy may occur, which involves the excessive excitation of

primary afferent receptors and central neurons, leading to pain, and other adverse effects (4). The activation of satellite glial cells (SGCs) has been reported to be an essential factor in several experimental models of pain (5-7). Hyperglycemia and dyslipidemia are hallmark features of pre-diabetes (8,9). Obesity-associated dysregulation of glucose and lipid metabolism has been associated with diabetes, and high blood sugar and free fatty acids (FFA) in serum are thought to contribute to neurological disorder development (10,11). Thus, cell injury inducing a high glucose high free fatty acid (HGHF) environment may effectively model the condition of neurological disorders in T2DM (12,13).

Adenosine 5'-triphosphate (ATP) is an important messenger that is involved in numerous processes, including the transmission of pain signals. It may also act as an acute pro-inflammatory danger signal and a crucial mediator of neuroinflammation. In an environment of inflammation or stress, levels of extracellular ATP (eATP) rapidly approach near millimolar levels and become the main stimulation of pro-inflammatory pathways (14). Subclasses of purinergic 2 (P2) receptors include P2X and P2Y. P2X receptors, particularly the P2X purinoceptor 7 (P2X$_7$), are strongly associated with immunity and inflammation (14). P2X$_7$ receptors are highly expressed in immune cells and are activated as a result of pro-inflammatory cytokine release (15). In SGCs, eATP may activate the P2X$_7$ receptor, thus possibly contributing to the development of chronic inflammatory disease (16).

Long non-coding RNAs (lncRNAs) are non-protein-coding RNA transcripts >200 nucleotides in length. Increasing evidence has highlighted the role of lncRNAs in physiology and disease (17,18). LncRNAs are involved in diverse regulatory processes, including the alteration of chromatin and transcriptional state, nuclear architecture, splicing and mRNA translation (19,20). LncRNA BC168687 is evolutionarily conserved across numerous species and significantly increased levels have been detected in the dorsal root ganglion (DRG) of type 2 diabetic rats (21). Therefore, BC168687 was selected for examination. The present study revealed that lncRNA BC168687 small interfering RNA (siRNA) may downregulate P2X$_7$ receptor expression induced by a HGHF environment in primary cultured SGCs.

Correspondence to: Dr Chang-Shui Xu, Department of Physiology, Basic Medical College of Nanchang University, 461 Bayi Avenue, Nanchang, Jiangxi 330006, P.R. China
E-mail: xuchangshui@ncu.edu

Materials and methods

Primary culture. The present study was approved by the Ethical Committee of Nanchang University (Nanchang, China) and animals were treated according to the Guidelines for the Care and Use of Animals (22). Fetal Sprague-Dawley rats (n=6; male; 7-9 g) were obtained from the Laboratory Animal Science Department of Nanchang University (Nanchang, China). All rats were housed in clean, standard metabolic cages and kept at a constant temperature of 37°C with 35-65% humidity. The rats were kept in a 12 h light/dark cycle and had free access to food and water. On the third day, rats were anesthetized using ether. The DRGs of fetal rats were extracted with microforceps and rapidly transferred into Dulbecco's modified Eagle Medium/F12 (DMEM/F12) medium (HyClone; GE Healthcare Life Sciences, Logan, UT, USA) and incubated at 4°C for 30 min prior to the next step. Following the detachment of redundant fibers with ophthalmic forceps, the DRGs were incubated with collagenase type III (0.1 mg/ml; Beijing Solarbio Science and Technology, Ltd., Beijing, China) for 15 min at 37°C. The collagenase was removed by centrifugation at 168 x g for 5 min and DRGs were pre-incubated with 0.25% trypsin-EDTA (0.5 mg/ml; Beijing Solarbio Science and Technology, Ltd.) in a cell incubator for 35-40 min at 37°C. DMEM/F12 containing 10% fetal bovine serum (FBS; Biological Industries, Kibbutz Bei-Haemek, Israel) was subsequently used to terminate enzymatic digestion.

The DRGs were blown gently using sterile disposable pipettes before being passed through a cell strainer (aperture, 70 μm; 200 mesh). Glial cells (5x10^5 cells/ml) were inoculated on polylysine-coated coverslips into 24-well plates to obtain cell climbing slides. SGCs were purified from glial cells by replacing the medium twice every 24 h. The purified SGCs were sustained in DMEM/F12 containing 10% FBS (Biological Industries), 100 U/ml penicillin and 100 mg/ml streptomycin sulfate at 37°C in a humidified incubator with 5% CO$_2$. To imitate hyperglycemia and dyslipidemia, 40 mM D-glucose (Beijing Solarbio Science and Technology, Ltd.) and 0.60 mM FFAs were added to DMEM/F12 medium. FFAs were a mixture of oleate (Sigma-Aldrich; Merck KGaA, Darmstadt, Germany) and palmitate (Sigma-Aldrich, Merck KGaA) at a 2:1 ratio (w/w) (23,24). In addition, 20 mM D-Mannitol (Beijing Solarbio Science and Technology) was added into DMEM/F12 as an isotonic control.

SGCs were divided into five groups: Control, HGHF (40 mM D-glucose and 0.60 mM FFAs), HGHF+BC168687 small interfering RNA (siRNA), HGHF+negative control siRNA (NCsi) and HGHF+empty vector control (VD; Entranster™-R4000; Engreen Biosystem, Ltd., Beijing, China). SGCs were treated with HGHF for 72 h. When the cells reached 70-80% confluence, siRNAs (50 nM) were transfected into SGCs in 24-well plates for further experimentation.

siRNA transfection. The following BC168687 siRNA and negative control siRNA sequences were synthesized (Novobio Scientific, Inc., Shanghai, China) and used: BC168687-rat-159 (5'-GAGAUUAUUAAGGUGUAC UTT-3'), BC168687-rat-1172 (5'-GACGGUUGAUAC UGACUCUTT-3'), BC168687-rat-2400 (5'-GUUGGA UCCUUCUCAAUCATT-3') and negative control siRNA (5'-UUCUCCGAACGUGUCACGUTT-3'). The three different BC168687 siRNA duplexes were transfected into SGCs using the Entranster™-R4000 (Engreen Biosystem, Ltd.) according to the manufacturer's protocol. After 48 h, the expression levels of BC168687 were evaluated by reverse transcription quantitative-polymerase chain reaction (RT-qPCR).

Cell viability test. The viability of SGCs was analyzed with the TransDetect Cell Counting kit (CKK; Beijing TransGen Biotech, Co., Ltd., Beijing, China). A suspension of 100 μl SGCs (5x10^3 cells/ml) from each group was placed onto a 96-well microplate. Each group was tested in triplicate. Following culture of SGCs at the different concentrations of D-glucose and FFA for 72 h, 10% CCK diluent was added to each well. Cells were subsequently maintained in a cell incubator for 2 h. A wavelength of 450 nm was used to detect the absorbance using a multimode plate reader. The data was analyzed with GraphPad Prism v6.0 (GraphPad Software Inc., La Jolla, CA, USA).

RT-qPCR. RNA was extracted with Transzol Up (Beijing TransGen Biotech, Ltd.) and reverse transcribed at 37°C for 1 h using a RevertAid™ First Strand cDNA Synthesis kit (Thermo Fisher Scientific, Inc., Waltham, MA, USA). The concentration of cDNA for each group was detected to be ~4x10^3 ng/μl using the NanoDrop2000 (Thermo Fisher Scientific, Inc.). The primer sequences used (Sangon Biotech Co., Ltd., Shanghai, China) were as follows: BC168687 forward, 5'-GGACAAGTC CTTAGCCATGC-3' and reverse, 5'-CAACACCGTTGGATC CTTCT-3'; P2X$_7$ forward, 5'-GCACGAATTATGGCACCG TC-3' and reverse, 5'-CCCCACCCTCTGTGACATTC-3'; and β-actin forward, 5'-CCTAAGGCCAACCGTGAAAAGA-3' and reverse, 5'-GGTACGACCAGAGGCATACA-3'. RT-qPCR was performed using the SYBR Premix Ex Taq (Takara Biotechnology Co., Ltd., Dalian, China) and the StepOnePlus™ Real-Time PCR system (Thermo Fisher Scientific, Inc.). The thermo cycling conditions were as follows: 95°C for 30 sec, 60°C for 15 sec, 95°C for 15 sec, 60°C for 1 min and 95°C for 15 sec. The melting curve was used to determine the amplification specificity and results were analyzed using the StepOnePlus Real-Time PCR system. The average threshold cycle (Cq) value for the target minus the average value for β-actin was used to calculate the ΔCq value (ΔCq=Cq target-Cq reference). The ΔΔCq value was calculated as follows: ΔCq test sample-ΔCq calibrator sample. The relative quantity (RQ) of the gene expression was calculated using the following equation: 2$^{-\Delta\Delta Cq}$ (21).

Immunocytochemistry. Immunocytochemistry was performed with the SPlink Detection kit (cat no. SP-9001; OriGene Technologies, Inc., Beijing, China) and the working solutions provided by the manufacturer were used if not otherwise specified. Cell climbing slides (diameter, 8 mm) were removed from DMEM/F12 and washed three times in PBS and subsequently fixed in 4% paraformaldehyde (Beijing Solarbio Science and Technology, Ltd.) for 15 min at room temperature. Following three washes with PBS, slides were blocked with normal goat serum at 37°C for 30 min. The slides were washed in PBS and incubated with P2X$_7$ primary antibody (cat no. APR-004-AO; 1:200; Alomone Labs, Jerusalem, Israel) overnight at 4°C.

Slides were washed in PBS and incubated with Biotin labeled goat anti-rabbit IgG polymer secondary antibody for 15 min at 37˚C. Slides were washed again with PBS prior to incubation with alkaline phosphatase-labeled streptavidin for 15 min at 37˚C. Slides were subsequently stained with 3,3'-diamino-benzindine solution (OriGene Technologies, Inc.) at room temperature for 10 min and sealed by neutral balsam (OriGene Technologies, Inc.). The expression of $P2X_7$ receptors was visualized with a fluorescence inverted microscope (magnification, x200) and the integrated optical density (IOD) of the $P2X_7$ receptors was calculated using Image-Pro Plus v6.0 (Media Cybernetics Inc., Rockville, MD, USA).

Western blot analysis. SGCs total protein was extracted with the Mammal Cell Protein Extraction reagent (Wuhan Boster Biological Technology, Ltd., Wuhan, China). Protein concentrations were detected with a multimode plate reader using a Bradford Protein Assay kit (Beyotime Institute of Biotechnology, Shanghai, China). Supernatant samples containing 20 μg of protein were separated by 10% SDS-PAGE and transferred onto polyvinylidene fluoride (PVDF) membranes. The PVDF membranes were blocked in 5% bovine serum albumin (Beijing Solarbio Science and Technology, Ltd.) at room temperature for 2 h and subsequently incubated with the following primary antibodies overnight at 4˚C: rabbit anti-$P2X_7$ (cat. no. APR-004-AO; dilution, 1:500; Alomone Labs), mouse anti-glial fibrillary acidic protein (GFAP; cat. no. 644701; dilution, 1:200; BioLegend, Inc., San Diego, CA, USA), rabbit anti-phosphorylated-extracellular signal-related kinase 1/2 (ERK1/2) (Thr202/Thr204) (cat. no. D13.24.4E; dilution, 1:1,000; Cell Signaling Technology, Inc. Danvers, MA, USA), rabbit anti-ERK1/2 (cat. no. 137F5; dilution, 1:1,000; Cell Signaling Technology, Inc.), and mouse anti-β-actin antibody (cat. no. TA-09l; dilution, 1:800; OriGene Technologies, Inc.). The following day membranes were washed three times with TBST and incubated with the following secondary antibodies: Peroxidase-conjugated goat anti-rabbit IgG (1:2,000; cat no. ZB-2301; OriGene Technologies, Inc.) and goat anti-mouse IgG (1:2,000; cat no. ZB-2305; OriGene Technologies, Inc.) for 2 h at room temperature. Bands were visualized using the Enhanced Chemiluminescent reagent kit (Wuhan Boster Biological Technology, Ltd.) and the IOD was calculated using Image-Pro Plus v6.0 (Media Cybernetics Inc.).

Double immunofluorescence. Cell climbing slides (diameter, 8 mm) were removed from DMEM/F12 and washed three times with PBS. Slides were fixed with 4% paraformaldehyde (Beijing Solarbio Science and Technology, Ltd.) for 15 min at room temperature. Slides were washed three times in PBS and subsequently blocked with normal goat serum (OriGene Technologies, Inc.) at the working solution provided by the manufacturer for 1 h in a thermostatic water bath at 37˚C, prior to incubation with rabbit anti-$P2X_7$ (cat. no. APR-004-AO; dilution, 1:200; Alomone Labs) and mouse anti-GFAP (cat. no. 644701; dilution, 1:200; BioLegend, Inc.) overnight at 4˚C. Slides were then washed three times with PBS, and incubated with fluorescent goat anti-mouse fluorescein isothiocyante (1:200; cat no. ZF-0311; OriGene Technologies, Inc.) and goat anti-rabbit tetramethylrhodamine isothiocyanate secondary antibodies (1:200; cat no. ZF-0313; OriGene Technologies, Inc.) in the dark at 37˚C for 1 h. Slides were washed three times with PBS and subsequently stained with DAPI (cat. no. AR1176; dilution, 1:1,000; Wuhan Boster Biological Technology, Ltd.) at 37˚C for 60 sec. Slides were washed three times with PBS, sealed with anti-fluorescent quencher (Wuhan Boster Biological Technology, Ltd.) and visualized with a fluorescence inverted microscope.

Measurement of eATP. The release of ATP from SGCs was measured using an ATPlite 1 step luminescence assay system kit (10 ml; PerkinElmer, Inc., Waltham, MA, USA). A suspension of 100 μl SGCs from each group was placed onto a 96-well microplate. Each group was tested in triplicate. The substrate vial and buffer solution were equilibrated at room temperature. The lyophilized substrate solution was then mixed with the buffer and left to stand at room temperature for 5 min. The reconstituted reagent (100 μl) was subsequently added into each well containing the 100 μl suspension. The 96-well microplates were agitated for 2 min at 168 x g at 37˚C and the luminescence was measured using a multimode plate reader.

Measurement of intracellular nitric oxide (NO) and ROS. Intracellular NO was measured using the nitrate reductase method (21). The NO concentration in each group was calculated according to the formula provided in the Nitric Oxide Assay kit (Nanjing Jiancheng Bioengineering Institute, Nanjing, China). The IOD values of each group were calculated using a multimode plate reader.

Intracellular ROS levels were inspected with the ROS Assay kit (Nanjing KeyGen Biotech Co., Ltd., Nanjing, China). Following the removal of DMEM/F12 from SGCs, diluted 2',7'-dichlorofluorescin diacetate (DCFH-DA; 1:1,000; 10 μM; cat no. S0033, Beyotime Institute of Biotechnology) was added. Sample were placed into 24-well plates and incubated for 20 min at 37˚C, then subsequently washed three times with serum-free DMEM/F12. The fluorescence density was detected at an excitation wavelength of 488 nm and an emission wavelength of 525 nm with the multimode plate reader.

Statistical analysis. Results are presented as the mean ± standard error. GraphPad Prism v6.0 (GraphPad Software Inc.) and Image-Pro Plus v6.0 (Media Cybernetics Inc.) were used to perform the statistical tests. The unpaired Student's t-test was used when comparing two groups and the one-way analysis of variance with the Bonferroni correction was used for multiple comparisons. $P<0.05$ was considered to indicate a statistically significant difference.

Results

Screening of high D-glucose and FFAs concentrations. SGC viability was measured with CCK. The results indicated that the viability of SGCs in a D-glucose environment significantly decreased at D-glucose concentrations of ≥40 mM: Control, 0.49±0.02; isotonic control, 0.50±0.02; 10 mM D-glucose; 0.48±0.02; 20 mM D-glucose, 0.48±0.01; 40 mM D-glucose,
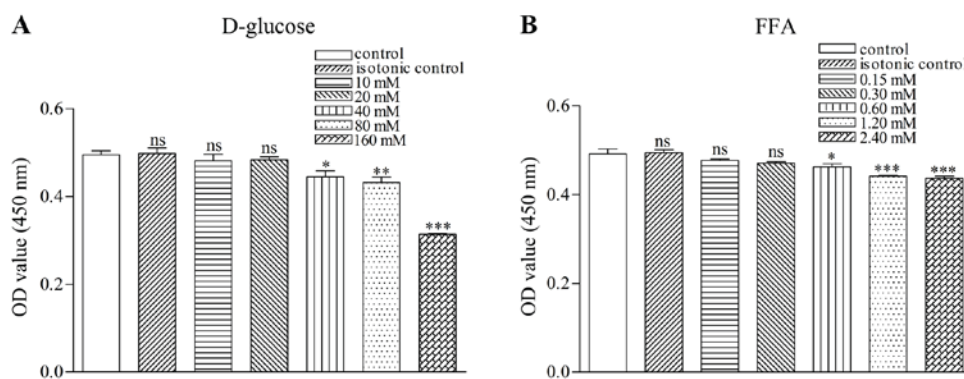
Figure 1. Effect of increasing (A) D-glucose and (B) FFA concentrations on cell viability as detected by the TransDetect Cell Counting kit. *P<0.05, **P<0.01, ***P<0.001 vs. control group. ns, no significant difference; OD, optical density; FFA, free fatty acid.
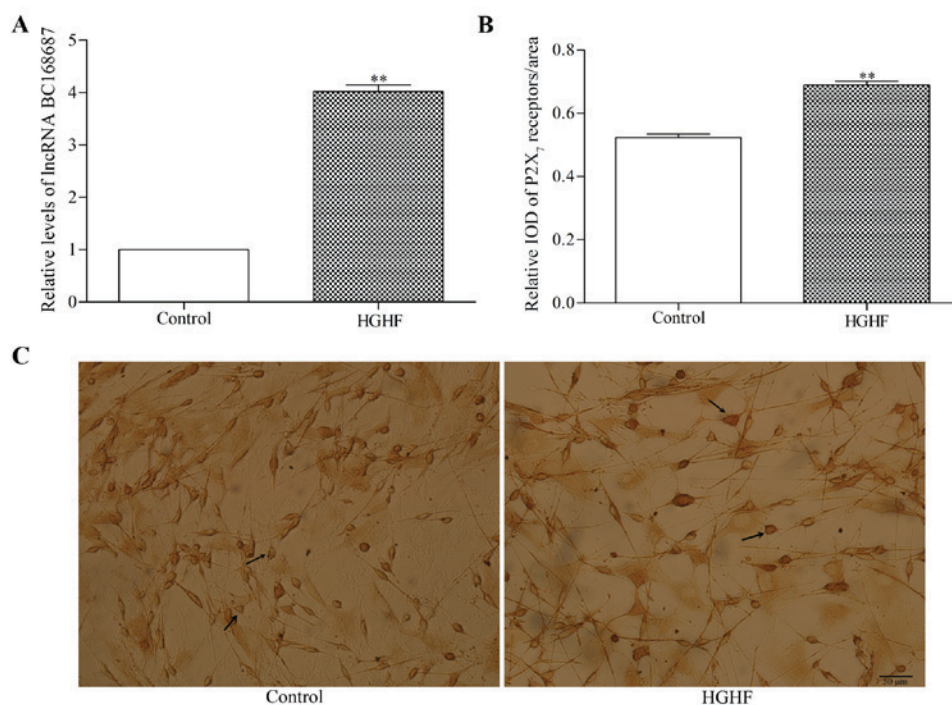

Figure 2. HGHF upregulates BC168687 and P2X$_7$ receptor expression in primary cultured SGCs. (A) The relative expression levels of BC168687 and (B) P2X$_7$ receptors in HGHF-induced SGCs was determined by reverse transcription quantitative-polymerase chain reaction. (C) P2X$_7$ receptor expression in SGCs was visualized by immunocytochemistry. The arrows indicate the positive SGCs. Scale bar, 50 μm. **P<0.01 vs. control group. P2X$_7$, P2X purinoceptor 7; HGHF, high glucose and high free fatty acids; SGC, satellite glial cell; lncRNA, long noncoding RNA; IOD, integrated optical density.

0.45±0.02; 80 mM D-glucose, 0.43±0.02; and 160 mM D-glucose 0.31±0.00 (Fig. 1A).

The viability of SGCs in a FFA environment was also significantly decreased at FFA concentrations ≥0.60 mM: Control, 0.49±0.02; isotonic control, 0.49±0.01; 0.15 mM, 0.48±0.01; 0.30 mM, 0.47±0.00; 0.60 mM, 0.46±0.01; 1.2 mM, 0.44±0.01; and 2.4 mM, 0.44±0.02 (Fig. 1B). Based on the aforementioned results, 40 mM D-glucose and 0.6 mM FFA were selected as the final concentrations to produce a HGHF environment.

P2X$_7$ receptor and lncRNA BC168687 expression in SGCs in a HGHF environment. The relative expression level of BC168687 was determined using RT-qPCR (Fig. 2A) and the expression of P2X$_7$ receptors was analyzed with immunocytochemistry

(Fig. 2B and C). The results indicated that the relative expression levels of BC168687 and P2X$_7$ were higher in the HGHF environment compared with the control group (Fig. 2A and B; P<0.01).

BC168687 siRNA screening and P2X$_7$ mRNA expression in SGCs. Following the transfection of siRNAs into SGCs for 48 h, duplexes from three different siRNA sequences were screened for effective BC168687 silencing (Fig. 3A). The relative level of BC168687 and P2X$_7$ mRNA expression in SGCs was determined using RT-qPCR (Fig. 3B). The results revealed that the relative level of BC168687 was significantly decreased by siRNAs 1172 (P<0.05) and 2400 (P<0.001): Control, 1.00±0.00; BC168687-159si, 0.83±0.08; BC168687-1172si, 0.75±0.19; BC168687-2400si, 0.56±0.04.
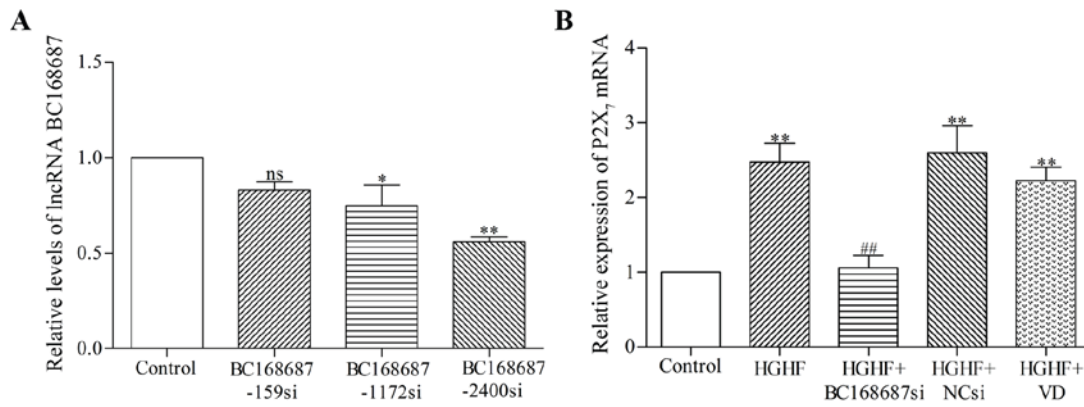
Figure 3. BC168687 siRNA and P2X$_7$ mRNA expression in SGCs was determined by reverse transcription quantitative-polymerase chain reaction. (A) Three different BC168687 siRNAs were transfected in order to determine the most effective silencing sequence. BC168687 was selected. (B) P2X$_7$ mRNA expression in the HGHF group was increased compared with the control group and P2X$_7$ mRNA expression in the BC168687si group was decreased compared with the HGHF group. *P<0.05, **P<0.01 vs. control group. ##P<0.01 vs. HGHF group. siRNA, small interfering RNA; SGC, satellite glial cell; P2X$_7$, P2X purinoceptor 7; HGHF, high glucose and free fatty acids; NCsi, negative control siRNA; ns, no significant difference; lncRNA, long noncoding RNA; VD, empty vector control.
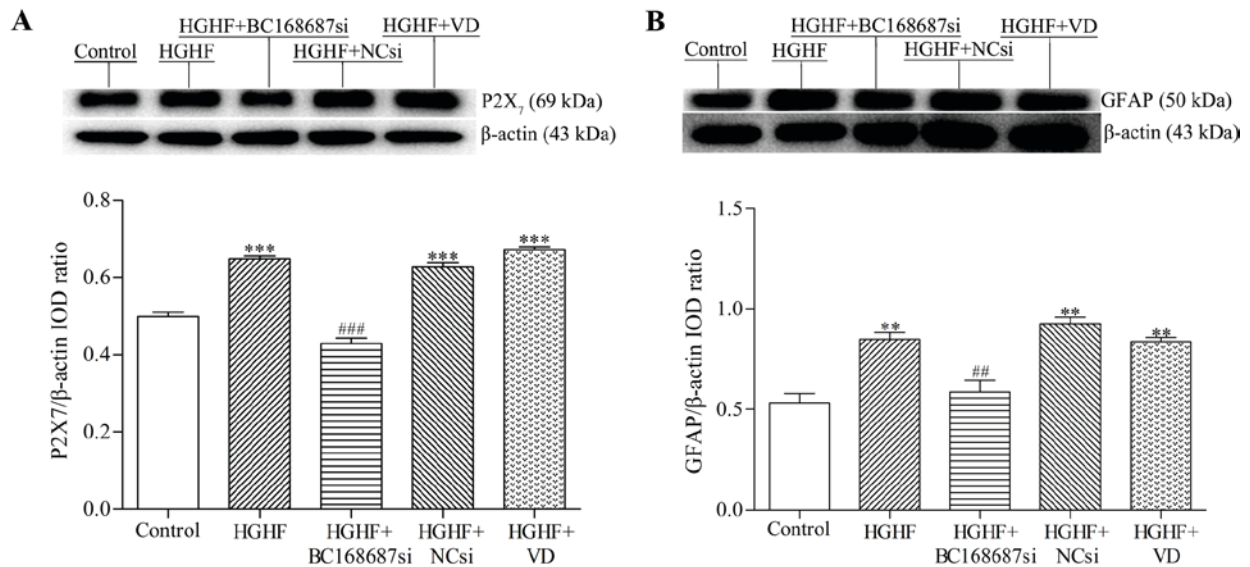

Figure 4. BC168687 siRNA downregulates the expression of P2X$_7$ and GFAP induced by HGHF in SGCs. (A) Representative western blot analysis and the relative expression levels of P2X$_7$ and (B) GFAP. β-actin from the same sample was used as an internal control. The expression of P2X$_7$ protein and GFAP in the HGHF group was significantly increased compared with the control group. The expression levels of P2X$_7$ protein and GFAP in the BC168687si group significantly decreased compared with the HGHF group. **P<0.05, ***P<0.001 vs. Control group. ##P<0.05, ###P<0.001 vs. HGHF group. siRNA, small interfering RNA; P2X$_7$, P2X purinoceptor 7; GFAP, glial fibrillary acidic protein; HGHF, high glucose and high free fatty acids; SGC, satellite glial cell; NCsi, negative control siRNA; IOD, integrated optical density; VD, empty vector control.

Thus, BC168687-2400 was selected as the targeting siRNA of BC168687.

The relative mRNA expression of P2X$_7$ in each group was as follows: Control, 1.00±0.00; HGHF, 2.47±0.44; HGHF+BC168687si, 1.06±0.29; HGHF+NCsi, 2.60±0.64; and HGHF+VD, 2.23±0.31. The variance was statistically significant (P<0.01). Compared with the control group, P2X$_7$ mRNA expression in the HGHF group was significantly increased. P2X$_7$ mRNA expression in the HGHF+BC168687si group was significantly lower compared with the HGHF group (P<0.01). No significant differences were observed among the HGHF, HGHF+NCsi and HGHF+VD group. Based on the results obtained, it was concluded that BC168687 siRNA was able to

attenuate the upregulation of P2X$_7$ mRNA induced in a HGHF environment.

BC168687 siRNA downregulates the expression of P2X$_7$ and GFAP in SGCs. Following transfection of the siRNAs into SGCs for 72 h, P2X$_7$ and GFAP expression was detected by western blot analysis (Fig. 4A and B). The relative expression of P2X$_7$ in each group was as follows: Control, 0.50±0.02; HGHF, 0.65±0.01; HGHF+BC168687si, 0.43±0.03; HGHF+NCsi, 0.63±0.02 and HGHF+VD 0.67±0.01. The variance analysis was statistically significant between the HGHF+BC168687si and HGHF group (P<0.001). The relative expression of GFAP in each group was as follows: Control,
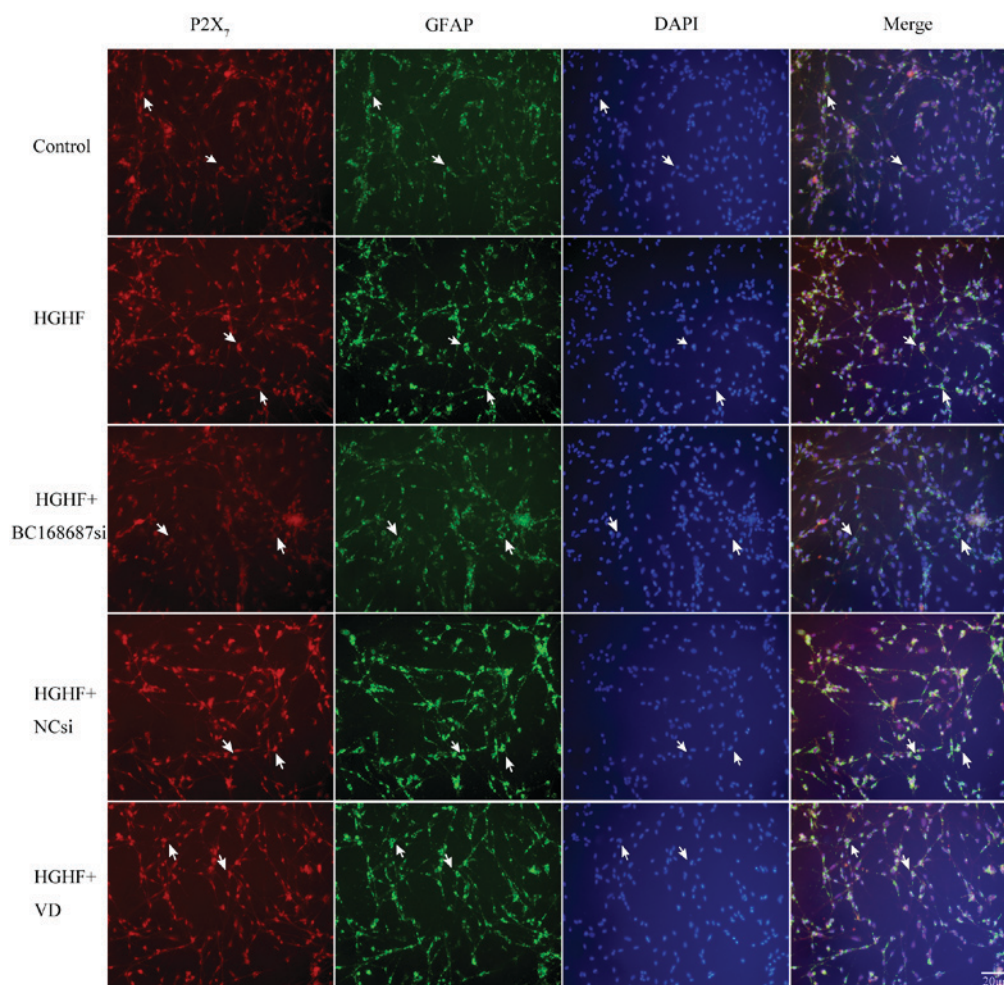
Figure 5. P2X$_7$ and GFAP co-expression was increased in SGCs in a HGHF environment. The co-expression of P2X$_7$ receptor and GFAP in the HGHF group was increased compared with the control group, whereas the co-expression value in the BC168687si group was decreased compared with the HGHF group. The green signal indicates GFAP staining with fluorescein isothiocyante. The red signal indicates P2X$_7$ staining with tetramethylrhodamine isothiocyanate; the blue signal indicates nucleus staining with DAPI. The arrows indicate the positive SGCs. Scale bar, 20 μm. P2X$_7$, P2X purinoceptor 7; GFAP, glial fibrillary acidic protein; HGHF, high glucose and high free fatty acids; SGC, satellite glial cell; NCsi, negative control siRNA; VD, empty vector control.

0.53±0.08; HGHF, 0.85±0.06; HGHF+BC168687si, 0.59±0.10; HGHF+NCsi, 0.93±0.05; and HGHF+VD, 0.84±0.04. Expression of P2X$_7$ protein and GFAP in the HGHF group was signficantly increased compared with the control group (P<0.01). Compared with the HGHF group, the P2X$_7$ protein and GFAP expression levels were signficantly decreased in the HGHF+BC168687si group (P<0.01). No significant differences were observed among the HGHF, HGHF+NCsi and HGHF+VD groups. Therefore, BC168687 siRNA may attenuate the upregulation of the P2X$_7$ receptor and GFAP induced by a HGHF environment in SGCs.

P2X$_7$ and GFAP co-expression is induced by a HGHF environment in SGCs. Immunofluorescence was used to detect the co-expression of P2X$_7$ receptor and GFAP in SGCs (25). The co-expression quantities of the P2X$_7$ receptors and GFAP in the five groups was detected following 72 h of siRNA transfection, based on the co-localization of P2X$_7$ and GFAP in SGCs (Fig. 5). Compared with the control group, the P2X$_7$ receptor and GFAP co-expression quantities were increased in the HGHF group. The co-expression quantities of the HGHF+BC168687si group were decreased compared with the

HGHF group. No apparent difference was observed among the HGHF, HGHF+NCsi and HGHF+VD groups. Therefore, it was inferred that BC168687 siRNA may reduce the P2X$_7$ receptor upregulation induced by a HGHF environment.

BC168687 siRNA reduces the upregulation of p-ERK1/2 expression induced by a HGHF environment in SGCs. The expression level of phosphorylated-ERK1/2 protein in SGCs was detected by western blot analysis. The relative expression levels of p-ERK1/2 protein in each group were as follows: Control, 0.50±0.02; HGHF, 0.58±0.02; HGHF+BC168687si, 0.52±0.10; HGHF+NCsi, 0.65±0.03; and HGHF+VD, 0.60±0.01. Compared with the control group, the p-ERK1/2 protein expression in the HGHF group was signficantly increased. The expression level of p-ERK1/2 protein in the HGHF+BC168687si group was significantly decreased compared with the HGHF group (Fig. 6A; P<0.01). No signifi-cant difference was observed among the HGHF, HGHF+NCsi and HGHF+VD groups. Based on the results obtained, it was concluded that BC168687 siRNA was able to reduce the upregulation of p-ERK1/2 signalling induced by a HGHF environment in SGCs.
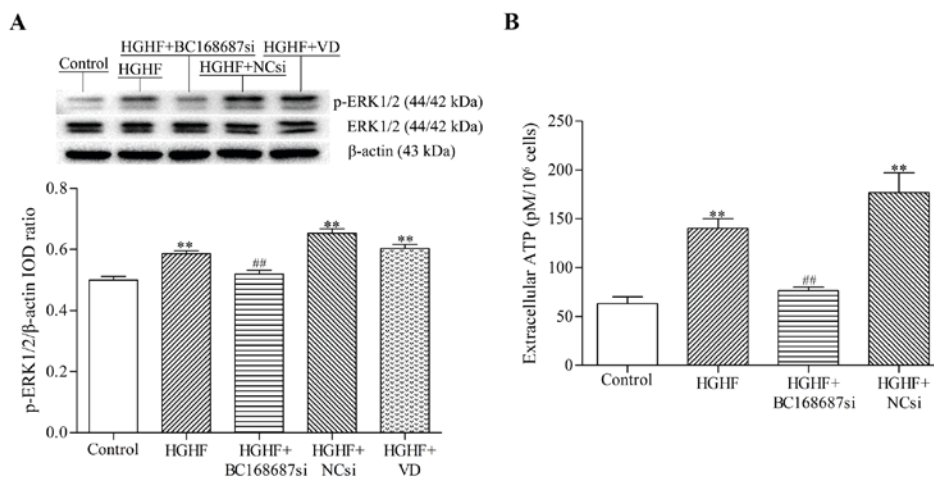
Figure 6. BC168687 siRNA reduced the level of p-ERK1/2 protein and ATP induced by HGHF in SGCs. (A) p-ERK1/2 protein expression levels in the HGHF group were increased compared with the control group and expression levels in the BC168687si group were decreased compared with the HGHF group (B) ATP levels in HGHF group were increased compared with the control group. ATP levels in the BC168687si group were decreased compared with the HGHF group. **P<0.01 vs. control group; ##P<0.01 vs. HGHF group. siRNA, small interfering RNA; p-, phosphorylated; ERK, extracellular signal-related kinase; ATP, adenosine 5'-triphosphate; HGHF, high glucose and high free fatty acids; SGC, satellite glial cell; NCsi, negative control siRNA; IOD, integrated optical density; VD, empty vector control.
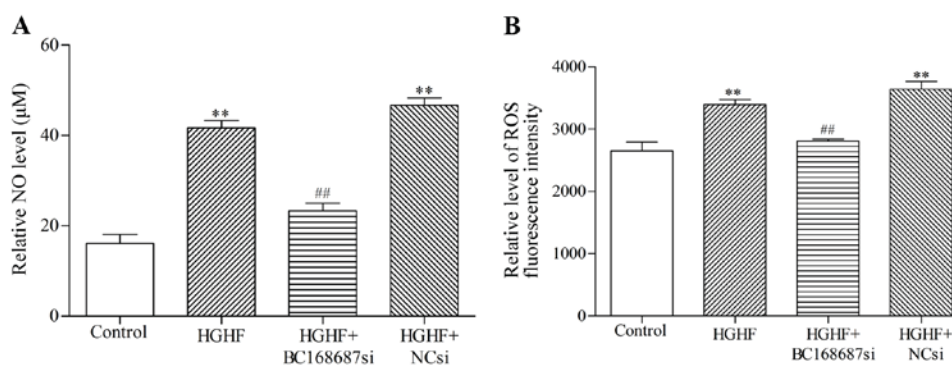

Figure 7. BC168687 siRNA reduced NO and ROS in SGCs in a HGHF environment. The levels of (A) NO and (B) ROS in HGHF group were increased compared with the control group. Levels of NO and ROS in the BC168687si group were decreased compared with the HGHF group. **P<0.01 vs. control group; ##P<0.01 vs. HGHF group. siRNA, small interfering RNA; NO, nitric oxide; ROS, reactive oxygen species; SGC, satellite glial cell; HGHF, high glucose and high free fatty acids; NCsi, negative control siRNA.

Effect of BC168687 siRNA on ATP levels in SGCs induced by a HGHF environment. As a proinflammatory mediator released from SGCs, ATP contributes to the initiation and maintainence of neuropathic pain (26). The results revealed that the concentrations of ATP (pM) in each group were as follows: Control, 63.33±11.55; HGHF, 140±17.32; HGHF+BC168687si, 76.67±5.77; and HGHF+NCsi, 176.67±35.12. ATP levels in the HGHF group were signficantly increased compared with the control group (Fig. 6B; P<0.01) and the levels of ATP in the HGHF+BC168687si group were significantly decreased compared with the HGHF group (P<0.01). There was no significant difference between the HGHF and HGHF+NCsi groups.

Effect of BC168687 siRNA on NO and ROS levels in SGCs induced by a HGHF environment. NO and ROS are oxidative injury factors released from SGCs that are also considered to contribute to the initiation and maintainence of neuropathic pain (27-29). The results revealed that the concentrations (μM)

of NO in each group were as follows: Control, 16.11±3.47; HGHF, 41.67±2.89; HGHF+BC168687si, 23.33±2.89; and HGHF+NCsi, 46.67±2.89 (Fig. 7A). The variance was statistically significant between the HGHF+BC168687si and HGHF group (P<0.01). Intracellular ROS levels were measured by fluorescence density. The results of the ROS assay kit were as follows: Control, 2,655±243.98; HGHF, 3,394±141.74; HGHF+BC168687si, 2,807±58.03; and HGHF+Ncsi, 3,642±213.18 (Fig. 7B). NO and ROS levels in the HGHF group were significantly increased compared with the control group (P<0.01). NO and ROS levels in the HGHF+BC168687 si group were signficantly decreased compared with the HGHF group (P<0.01). There was no signifcant difference between the HGHF and HGHF+NCsi groups.

Discussion

Compared with short-chain ncRNAs, including microRNAs, siRNAs and Piwi-interacting RNAs, lncRNAs account for the

majority of ncRNAs that regulate biological mechanisms and processes (30,31). They participate in the regulation of transcription and intracellular signal transduction pathways, including those involved in organism development (32). Therefore, dysregulated lncRNA expression may contribute to the development of numerous human diseases (33-35). P2X$_7$ receptors are expressed in SGCs and studies have demonstrated that P2X$_7$ receptors contribute to neuropathic pain (36-39). High levels of glucose and FFAs have been identified as a primary cause of nervous system dysfunction in diabetes (8,13). NcRNAs lack the ability to encode proteins, but possess regulatory functions, and are involved in almost all physiological and pathological processes (30,31,40-42). The present study demonstrated that BC168687 expression in SGCs in a HGHF environment group was significantly increased compared with the control group. P2X$_7$ receptor expression was also upregulated in SGCs in a HGHF environment, inferring the involvement of BC168687 in pathological processes mediated by P2X$_7$ receptors in SGCs.

The P2 receptor family is comprised of ligand-gated ion channel P2X receptors and G-protein coupled P2Y receptors (43). Autocrine release of ATP by glial cells activates P2X$_7$ receptors and may amplify pain signals through a cascade reaction (44-47). Thus, inhibiting P2X$_7$ receptors may relieve inflammatory and chronic neuropathic pain (37,39). The present study demonstrated that a HGHF environment increased ATP release in SGCs and BC168687 siRNA was able to decrease this release. P2X$_7$ mRNA and protein expression in SGCs in the HGHF group was significantly increased compared with the control group. Expression of P2X$_7$ mRNA and protein was significantly decreased in the HGHF+BC168687si group compared with the HGHF group, suggesting that BC168687 is associated with the upregulation of P2X$_7$ receptors observed in the HGHF group.

The increasing incidence of T2DM along with its comorbidities makes it urgent to understand the pathogenesis and regulatory mechanisms of the disease. The specific involvement of lncRNAs in diabetes is unclear (48,49). Diabetes is a chronic inflammatory disease, and the expression P2X$_7$ receptors may be upregulated by inflammatory injury (25,50). In an inflammatory state, ATP can be released from sensory neurons and SGCs in an autocrine or a paracrine fashion and activate P2 receptors (7,51). Excessive P2X$_7$ receptor excitation by ATP can promote the opening of plasma membrane pores, and may increase the release of pro-inflammatory cytokines, including interleukin-1β, interleukin-6 and tumor necrosis factor-α (37,52). These cytokines further induce glial cells to release pro-inflammatory mediators and exacerbate neuronal damage (14,45).

Oxidative stress is one of the important factors leading to diabetic neuropathy. Along with ATP, NO and ROS are released from glial cells and contribute to chronic neuropathic pain in diabetes (27,53,54). The present study indicated that HGHF significantly increased the release of NO and ROS, and these levels were decreased in the HGHF+BC168687si group. This suggests that BC168687 contributes to the pathological processes involving P2X$_7$ receptors, leading to neuropathic and peripheral inflammatory pain.

The mitogen-activated protein kinase (MAPK) signaling pathway is involved in cell proliferation, differentiation and adaptation, and may also contribute to the development of neuronal injury and disease. The MAPK family contains p38 MAPKs, ERK and c-Jun N-terminal kinases (55,56). The signaling pathways of MAPKs are crucial to signal transduction between neurons and glial cells, both of which are also essential for persistent pain (57,58). However, different MAPKs have distinct actions in glial cells following injury (58). Active ERK1/2 signaling occurs between the nucleus and the cytoplasm, and ROS is able to influence the ERK MAPK signaling pathway through phosphorylation (57,59). In the present study, an upregulation of p-ERK1/2 signaling was observed in SGCs in the HGHF group. Thus, it may be inferred that the ERK MAPK signaling pathway is involved in the aberrant activation of SGCs in a HGHF environment. Overall, it was concluded that BC168687 may be involved in the increased expression of P2X$_7$ receptors in SGCs in a HGHF environment, and BC168687 siRNA may have the potential to alleviate diabetic neuropathic pain mediated by P2X$_7$. These findings suggest BC168687 siRNA as a novel treatment for P2X$_7$ associated diseases including diabetic neuropathic pain. Further research to elucidate the specific mechanisms of BC168687 siRNA are required.

Acknowledgements

References

1. Szuszkiewicz-Garcia MM and Davidson JA: Cardiovascular disease in diabetes mellitus: Risk factors and medical therapy. Endocrinol Metab Clin North Am 43: 25-40, 2014.
2. Rathmann W and Giani G: Global prevalence of diabetes: Estimates for the year 2000 and projections for 2030. Diabetes Care 27: 2568-2569, 2004.
3. Katsiki N, Purrello F, Tsioufis C and Mikhailidis DP: Cardiovascular disease prevention strategies for type 2 diabetes mellitus. Expert Opin Pharmacother 18: 1243-1260, 2017.
4. Baron R: Peripheral neuropathic pain: From mechanisms to symptoms. Clin J Pain 16 (2 Suppl): S12-S20, 2000.
5. Wu JR, Chen H, Yao YY, Zhang MM, Jiang K, Zhou B, Zhang DX and Wang J: Local injection to sciatic nerve of dexmedetomidine reduces pain behaviors, SGCs activation, NGF expression and sympathetic sprouting in CCI Rats. Brain Res Bull 132: 118-128, 2017.
6. Ji RR, Chamessian A and Zhang YQ: Pain regulation by non-neuronal cells and inflammation. Science 354: 572-577, 2016.
7. Hanani M: Role of satellite glial cells in gastrointestinal pain. Front Cell Neurosci 9: 412, 2015.
8. Xu H, Wu B, Jiang F, Xiong S, Zhang B, Li G, Liu S, Gao Y, Xu C, Tu G, *et al*: High fatty acids modulate P2x(7) expression and Il-6 release via the P38 Mapk pathway in Pc12 cells. Brain Res Bull 94: 63-70, 2013.
9. Namekawa J, Takagi Y, Wakabayashi K, Nakamura Y, Watanabe A, Nagakubo D, Shirai M and Asai F: Effects of high-fat diet and fructose-rich diet on obesity, dyslipidemia and hyperglycemia in the Wbn/Kob-Lepr(Fa) rat, a new model of type 2 diabetes mellitus. J Vet Med Sci 79: 988-991, 2017.
10. Ruan X: Long Non-Coding Rna central of glucose homeostasis. J Cell Biochem 117: 1061-1065, 2016.

11. Kornfeld JW, Baitzel C, Könner AC, Nicholls HT, Vogt MC, Herrmanns K, Scheja L, Haumaitre C, Wolf AM, Knippschild U, *et al*: Obesity-induced overexpression of miR-802 impairs glucose metabolism through silencing of Hnf1b. Nature 494: 111-115, 2013.
12. Fan B, Gu JQ, Yan R, Zhang H, Feng J and Ikuyama S: High glucose, insulin and free fatty acid concentrations synergistically enhance perilipin 3 expression and lipid accumulation in macrophages. Metabolism 62: 1168-1179, 2013.
13. Singh H, Brindle NP and Zammit VA: High glucose and elevated fatty acids suppress signaling by the endothelium protective ligand angiopoietin-1. Microvasc Res 79: 121-127, 2010.
14. Burnstock G: P2x ion channel receptors and inflammation. Purinergic Signal 12: 59-67, 2016.
15. Baudelet D, Lipka E, Millet R and Ghinet A: Involvement of the P2x7 purinergic receptor in inflammation: An update of antagonists series since 2009 and their promising therapeutic potential. Curr Med Chem 22: 713-729, 2015.
16. Faria RX, Freitas HR and Reis RAM: P2x7 receptor large pore signaling in avian muller glial cells. J Bioenerg Biomembr 49: 215-229, 2017.
17. Kwok ZH and Tay Y: Long noncoding RNAs: Lincs between human health and disease. Biochem Soc Trans 45: 805-812, 2017.
18. Sun M and Kraus WL: From discovery to function: The expanding roles of long noncoding RNAs in physiology and disease. Endocr Rev 36: 25-64, 2015.
19. Wu Z, Liu X, Liu L, Deng H, Zhang J, Xu Q, Cen B and Ji A: Regulation of lncRNA expression. Cell Mol Biol Lett 19: 561-575, 2014.
20. Taylor DH, Chu ET, Spektor R and Soloway PD: Long non-coding RNA regulation of reproduction and development. Mol Reprod Dev 82: 932-956, 2015.
21. Liu C, Tao J, Wu H, Yang Y, Chen Q, Deng Z, Liu J and Xu C: Effects of LncRNA BC168687 SiRNA on diabetic neuropathic pain mediated by P2X7 receptor on SGCs in DRG of rats. Biomed Res Int 2017: 7831251, 2017.
22. Jones-Bolin S: Guidelines for the care and use of laboratory animals in biomedical research. Curr Protoc Pharmacol Appendix 4: Appendix 4B, 2012.
23. Hirose H, Lee YH, Inman LR, Nagasawa Y, Johnson JH and Unger RH: Defective fatty acid-mediated beta-cell compensation in Zucker diabetic fatty rats. pathogenic implications for obesity-dependent diabetes. J Biol Chem 271: 5633-5637, 1996.
24. Xu H, He L, Liu C, Tang L, Xu Y, Xiong M, Yang M, Fan Y, Hu F, Liu X, *et al*: LncRNA NONRATT021972 SiRNA attenuates P2X7 receptor expression and inflammatory cytokine production induced by combined high glucose and free fatty acids in PC12 Cells. Purinergic Signal 12: 259-268, 2016.
25. Liu S, Zou L, Xie J, Xie W, Wen S, Xie Q, Gao Y, Li G, Zhang C, Xu C, *et al*: LncRNA NONRATT021972 siRNA regulates neuropathic pain behaviors in type 2 diabetic rats through the P2X7 receptor in dorsal root ganglia. Mol Brain 9: 44, 2016.
26. Inoue K: Neuropharmacological study of ATP receptors, especially in the relationship between Glia and Pain. Yakugaku Zasshi 137: 563-569, 2017 (In Japanese).
27. Laursen JC, Cairns BE, Kumar U, Somvanshi RK, Dong XD, Arendt-Nielsen L, and Gazerani P: Nitric oxide release from trigeminal satellite glial cells is attenuated by glial modulators and glutamate. Int J Physiol Pathophysiol Pharmacol 5: 228-238, 2013.
28. Gwak YS, Hulsebosch CE and Leem JW: Neuronal-Glial interactions maintain chronic neuropathic pain after spinal cord injury. Neural Plast 2017: 2480689, 2017.
29. Chung MK, Asgar J, Lee J, Shim MS, Dumler C and Ro JY: The role of Trpm2 in hydrogen peroxide-induced expression of inflammatory cytokine and chemokine in rat trigeminal ganglia. Neuroscience 297: 160-169, 2015.
30. Taft RJ, Pang KC, Mercer TR, Dinger M and Mattick JS: Non-Coding RNAs: Regulators of disease. J Pathol 220: 126-139, 2010.
31. Ponting CP, Oliver PL and Reik W: Evolution and functions of long noncoding RNAs. Cell 136: 629-641, 2009.
32. Fitzgerald KA and Caffrey DR: Long noncoding RNAs in innate and adaptive immunity. Curr Opin Immunol 26: 140-146, 2014.
33. Lutz BM, Bekker A and Tao YX: Noncoding RNAs: New players in chronic pain. Anesthesiology 121: 409-417, 2014.
34. Wu P, Zuo X, Deng H, Liu X, Liu L and Ji A: Roles of long noncoding RNAs in brain development, functional diversification and neurodegenerative diseases. Brain Res Bull 97: 69-80, 2013.
35. Ma B, Gao Z, Lou J, Zhang H, Yuan Z, Wu Q, Li X and Zhang B: Long noncoding RNA MEG3 contributes to cisplatininduced apoptosis via inhibition of autophagy in human glioma cells. Mol Med Rep 16: 2946-2952, 2017.
36. Kobayashi K, Yamanaka H and Noguchi K: Expression of ATP receptors in the rat dorsal root ganglion and spinal cord. Anat Sci Int 88: 10-16, 2013.
37. Inoue K: P2 receptors and chronic pain. Purinergic Signal 3: 135-144, 2007.
38. Skaper SD, Debetto P and Giusti P: The P2x7 purinergic receptor: From physiology to neurological disorders. FASEB J 24: 337-345, 2010.
39. Sperlágh B, Vizi ES, Wirkner K and Illes P: P2x7 receptors in the nervous system. Prog Neurobiol 78: 327-346, 2006.
40. Amaral PP, Clark MB, Gascoigne DK, Dinger ME and Mattick JS: lncRNAdb: A reference database for long noncoding RNAs. Nucleic Acids Res 39 (Database Issue): D146-D151, 2011.
41. Maass PG, Luft FC and Bähring S: Long non-coding RNA in health and disease. J Mol Med (Berl) 92: 337-346, 2014.
42. Simionescu-Bankston A and Kumar A: Noncoding RNAs in the regulation of skeletal muscle biology in health and disease. J Mol Med (Berl) 94: 853-866, 2016.
43. Jarvis MF and Khakh BS: ATP-gated P2X cation-channels. Neuropharmacology 56: 208-215, 2009.
44. Caseley EA, Muench SP, Fishwick CW and Jiang LH: Structure-based identification and characterisation of structurally novel human P2X7 receptor antagonists. Biochem Pharmacol 116: 130-139, 2016.
45. Volonté C, Apolloni S, Skaper SD and Burnstock G: P2X7 receptors: Channels, pores and more. CNS Neurol Disord Drug Targets 11: 705-721, 2012.
46. Wei L, Caseley E, Li D and Jiang LH: ATP-induced P2X receptor-dependent large pore formation: How much do we know? Front Pharmacol 7: 5, 2016.
47. Dubyak GR: Go it alone no more-P2X7 joins the society of heteromeric ATP-gated receptor channels. Mol Pharmacol 72: 1402-1405, 2007.
48. Wu H, Yang L and Chen LL: The diversity of long noncoding RNAs and their generation. Trends Genet 33: 540-552, 2017.
49. Yan B, Yao J, Liu JY, Li XM, Wang XQ, Li YJ, Tao ZF, Song YC, Chen Q and Jiang Q: lncRNA-MIAT regulates microvascular dysfunction by functioning as a competing endogenous RNA. Circ Res 116: 1143-1156, 2015.
50. Peiró C, Lorenzo Ó, Carraro R and Sánchez-Ferrer CF: IL-1β inhibition in cardiovascular complications associated to diabetes mellitus. Front Pharmacol 8: 363, 2017.
51. Kojima S, Ohshima Y, Nakatsukasa H and Tsukimoto M: Role of ATP as a key signaling molecule mediating radiation-induced biological effects. Dose Response 15: 1559325817690638, 2017.
52. Lee JH, Zhang Y, Zhao Z, Ye X, Zhang X, Wang H and Ye J: Intracellular ATP in balance of pro- and anti-inflammatory cytokines in adipose tissue with and without tissue expansion. Int J Obes (Lond) 41: 645-651, 2017.
53. Blum E, Procacci P, Conte V and Hanani M: Systemic inflammation alters satellite glial cell function and structure. A possible contribution to pain. Neuroscience 274: 209-217, 2014.
54. Mima A: Inflammation and oxidative stress in diabetic nephropathy: New insights on its inhibition as new therapeutic targets. J Diabetes Res 2013: 248563, 2013.
55. Liu Y, Wang Z, Xie W, Gu Z, Xu Q and Su L: Oxidative stress regulates mitogenactivated protein kinases and c-Jun activation involved in heat stress and lipopolysaccharideinduced intestinal epithelial cell apoptosis. Mol Med Rep 16: 2579-2587, 2017.
56. Ji RR, Berta T and Nedergaard M: Glia and pain: Is chronic pain a gliopathy? Pain 154 (Suppl 1): S10-S28, 2013.
57. Ponnusamy M, Liu N, Gong R, Yan H and Zhuang S: ERK pathway mediates P2x7 expression and cell death in renal interstitial fibroblasts exposed to necrotic renal epithelial cells. Am J Physiol Renal Physiol 301: F650-F659, 2011.
58. Ji RR, Gereau RW IV, Malcangio M and Strichartz GR: MAP kinase and pain. Brain Res Rev 60: 135-148, 2009.
59. Son Y, Kim S, Chung HT and Pae HO: Reactive oxygen species in the activation of MAP kinases. Methods Enzymol 528: 27-48, 2013.